MATHEMATICAL MODELLING OF THE EFFECTIVENESS OF HELMETS IN HEAD PROTECTION

N.J. Mills and A. Gilchrist
Department of Metallurgy and Materials
University of Birmingham
Birmingham B15 2TT

F.J. Rowland
Health and Safety Executive
Sheffield

ABSTRACT

Computer models were developed for impacts on both Industrial Safety and Motorcycle Helmets. In these the masses of the helmet shell etc were assumed to act at a point and to move along one axis, whereas bending of the shell etc was modelled by springs plus dampers. When the model parameters were calculated from the measured behaviour of helmet elements, the predictions were in good agreement with theory. High speed photography confirmed the interpretation of impact events.

1 INTRODUCTION

There are several ways to improve the design of protective helmets. One is to modify constructional features such as the density of the shock-absorbing foam liner to see whether the peak acceleration in impact tests is reduced. However certain changes, such as the thickness of an injection moulded shell, are very expensive to make. A second method is to construct a simple mathematical model that duplicates the main features of the helmet impact response. It is then possible to optimise the performance by changing the values of the model parameter.

We have chosen to use a highly-simplified one-dimensional mathematical model, in which the material behaviour can be precisely specified. Such a model can be developed rapidly (1) and is economical in computing time. It can then be compared with a full analysis of instrumented impact tests (2) and high speed photography of the impacts. If the model is adequate then we can use it for optimisation. It also gives a physical insight into the ways in which loads are transferred from one part of the helmet to another and into the causes of force oscillations. If the model fails then we may need to use more complex finite element models (3) in which the full three-dimensional helmet geometry is incorporated. However it is difficult to incorporate dynamic effects in such finite element models.

2 CONSTRUCTION SITE WORKERS HELMETS

Standards and Materials

The British Standard for industrial safety helmets (4) defines such a helmet as "A helmet intended to protect primarily the upper part of a wearer's head against a blow from above'. Impact tests are carried out by dropping a 5 kg striker with a 50 mm radius hemispherical nose onto the top of the helmet. The striker has a kinetic energy of 49J at impact and its acceleration must not exceed 100 'g'.

The design of such helmets (fig. 1a) is dominated by the need to provide impact protection at the top. The thermoplastic shell can deform both by buckling inwards under the impact point, and by the thinner sides bending outwards. The plastics used, polyethylene, polypropylene or ABS, are viscoelastic so some energy is absorbed in the loading and unloading cycle. At the lower edge of the shell, the suspension cradle is mounted at 6 points. The cradle consists either of webbing straps or a flexible low density polyethylene moulding, and conveys the load back to the top of the head. The suspension can bend and stretch viscoelastically, and in severe impacts yields at its attachment points.

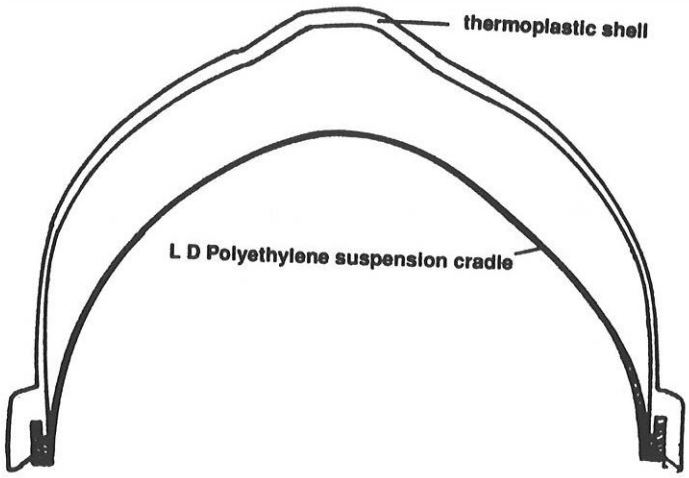

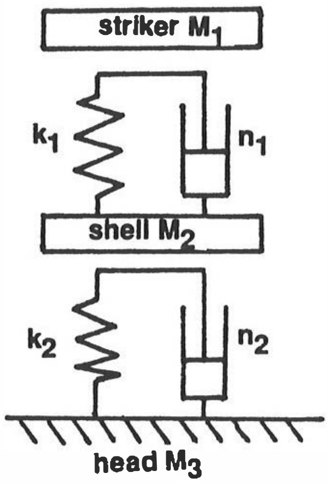

Fig. 1. Industrial safety helmet a) construction b) modelling for an impact on the top.

Modelling

Figure 1b shows the model used. The viscoelastic shell is in series with the viscoelastic suspension as the impact load is transmitted through the shell to the ends of the suspension cradle then through the cradle to the head. The position of the shell mass, typically 290 to 320 g, represents the centre of gravity of the shell. The shell mass is much smaller than the other two masses, and it tends to oscillate between them on the combined suspension of the two springs. The two spring constants were measured separately at low deformation rates, as k_1 = 300 to 400 kN/m for the bending of various shells and k_2 = 60 to 110 kN/m for the deformation of various suspension cradles. In principle the damper constants can be calculated from the coefficients of restitution measured for the various plastics (5), but initially the values were chosen empirically.

The sequence of computation steps was as follows:

i) from the positions x of the three masses the compressive deflections y of the spring/damper are calculated. If this is less than zero, loss-of-contact is assumed.

ii) the forces are calculated from the deflections y and the velocities V of the bodies. For example:

$$f_{12} = k_1 y_{12} + n_1 (V_2 - V_1)$$

gives the force between the striker and the shell masses. The suspension spring is non-linear (parabolic up to a force of 100 N) as this was observed in testing.

iii) the new accelerations a^* of the masses are calculaed using Newton's 3nd law, eg:

$$a_2^* = (f_{23} - f_{12})/m_2$$

iv) the clock is advancd by an interval Δt, typically 10 μs and the new velocities V^* of the bodies calculated by numerical integration. eg:

$$V_2^* = V_2 + 1/2\ (a_2 + a_2^*)\ \Delta t$$

where a_2 is the 'old' acceleration of mass 2.

v) a second numerical integration gives the new positions and the cycle of calculations restarts.

When the model predictions with parameters $k_1 = 300$, $k_2 = 110$ kN/m, $n_1 = 100$ $n_2 = 60$ Ns/m were compared with experimental data for a Protector Safety 'Tuffmaster II' helmet with an ABS shell and webbing cradle (fig. 2) there was found to be good agreement. The reasons for the oscillations in the striker force is that the shell mass of 0.3 kg oscillates on the combined spring of stiffness $k_1 + k_2 = 400$ kN/m; this leads to a natural frequency of about 200 Hz.

There is an initial impact in which the striker locally bends the helmet shell, and the striker force reaches the peak A (fig. 2). The shell mass then accelerates away from the striker and the local deformation of the top of the shell is seen to reduce to near zero; the striker force is a minimum at B. Next the suspension cradle decelerates the shell and the striker bends the top of the shell again. The second maximum in the striker force at C is when the striker is momentarily at rest, and both the shell and the suspension are fully deformed. Typically the deformation at this stage is 30 to 35 mm so the gap between the shell and the top of the headform is very small.

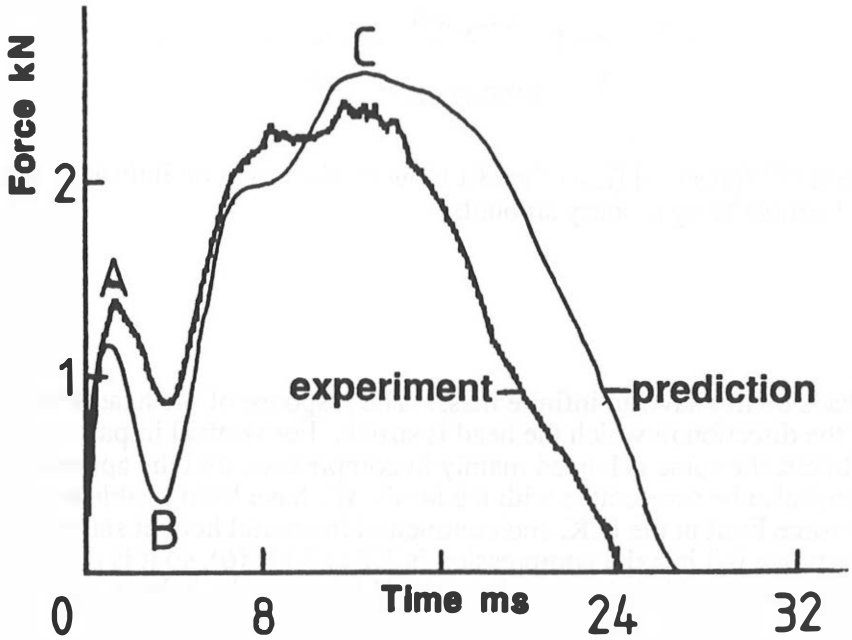

Fig. 2. Predicted vs experimental striker forces vs time for a 49 J blow of a hemispherical striker on the top of an industrial helmet (Tuffmaster II).

High Speed Photography

The photographic section of the HSE Laboratories took high speed film of impacts on the top of industrial helmets on 16 mm film at speeds in the range 1000 - 2000 frames/s. The 20 to 30 frames of interest were rephotographed onto 35 mm film and the prints measured. The frame speed was calculated from the observed striker speed prior to impact. The three measurements taken from the film were of the striker position, the position of the base of the helmet, and the local bending of the top of the helmet in contact with the hemispherical striker (fig. 3). The helmet was of a different make to that in fig. 2, but also had a thermoplastic shell. The data is straightforwrad to interpret until a time of 10 ms but after this the helmet began to rotate to the left as the striker slid off the marked central ridge of the helmet. Consequently when the data is compared with a computer simulation in fig.4 (for $k_1 = 500, k_2 = 200$ kN/m, $n_1 = 100, n_2 = 60$ Ns/m) the obseved striker rebound velocity is smaller than the predicted one. However the shell bending versus time is predicted well. The amount of bending falls to close to zero 2.5 ms after the initial impact as a result of the shell mass rebounding from the striker before any large force has built up in the suspension cradle.

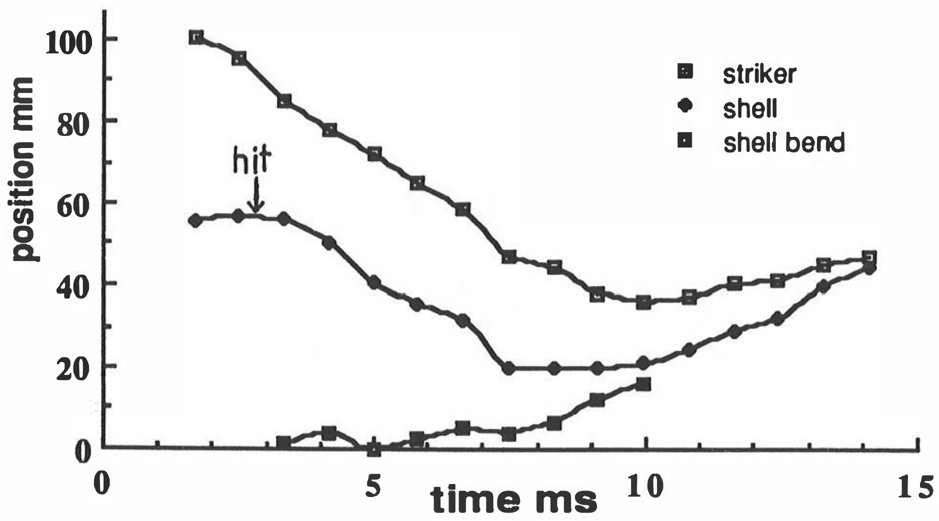

Fig. 3. Analysis of high speed film of a 98 J blow on the top of an industrial helmet - curves shifted vertically by arbitary amounts.

Discussion

In the real world heads do not have an infinite mass. The response of the head + neck + torso system depends on the direction in which the head is struck. For vertical impacts exactly on the top of industrial helmets, the spine is loaded mainly in compression and the approximately 30 kg mass of the torso must also be accelerated with the head. We have been unable to find the reason for the 5 kN striker force limit in the U.K. and continental industrial helmet standards. The force at which cervical vertibrae fail in axial compression is 3.7 to 5 kN (6), so it is possible that the helmet force criterion consider this injury mechanism. If however the helmet is hit on the front or side then the flexibility of the neck in bending means that the head acts as an independent 5 kg mass for the initial stages of the impact. If it is accepted that the head can tolerate up to 300 'g' linear acceleration, then for side or front impacts on industrial helmets the force on the headform should be less then 15 kN. We are currently working on the means to provide such side-impact protection in industrial helmets.

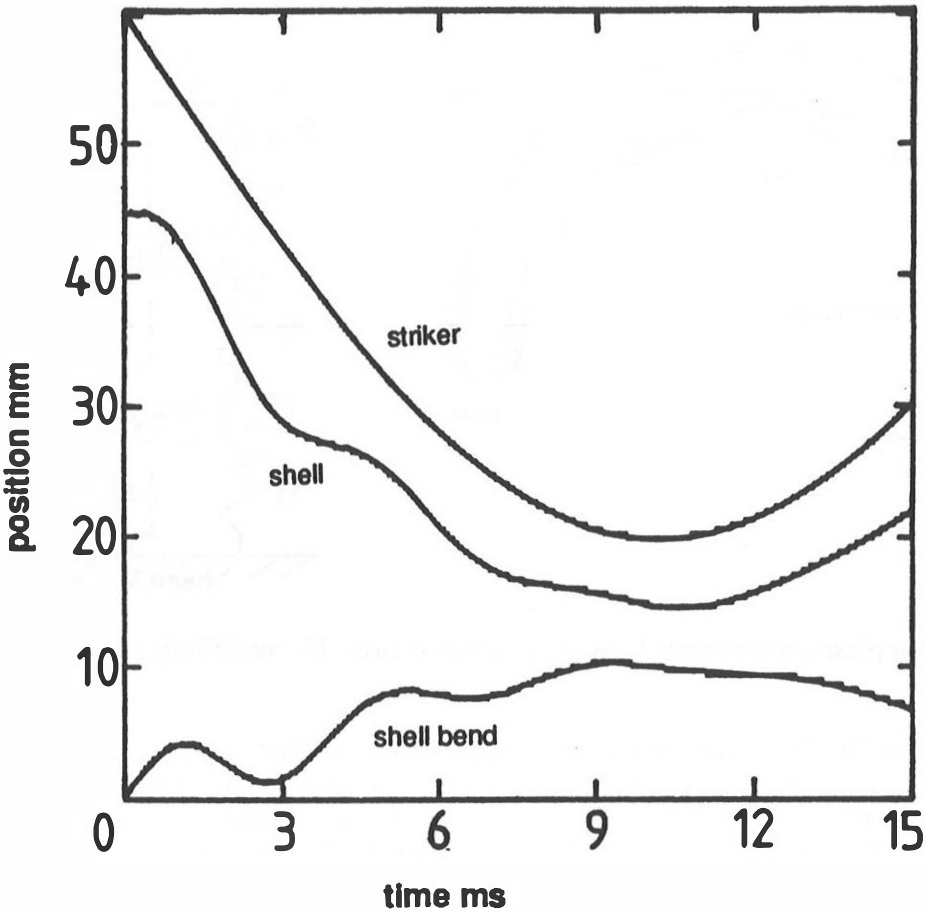

Fig. 4. Predicted positions of industrial helmet shell and striker for comparison with fig.3

3 MOTORCYCLE HELMETS

Materials and Design

The construction of a motorcycle helmet is far more complex (fig. 5a) than that of an industrial helmet. There are three main components, the shell, liner and comfort foam, and the material response of each will be considered separately.

The load transfer between the components is less obvious. When an impact causes the shell to bend inwards, the rigid shock-absorbing foam liner must deform by the same amount under the impact site. However loads can also be transmitted, as in industrial helmets, around to the base of the shell and through the uncrushed liner, which acts as a stiff suspension spring.

The shell can be made of thermoplastics, or of glass fibre reinforced thermosets. We assume that the former is used. The thermoplastic shells are thicker (4 to 5 mm) and of far more uniform thickness than in industrial helmets. They are also stiffened against bending by the presence of the liner.

Therefore the shell buckles inwards locally when impacted (7). Once the shell shape changes from being convex to being locally concave the stiffness falls. Figure 6a shows how this has been modelled to duplicate experimental data: the shell spring constant k_{1a} falls to a lower value k_{1b}

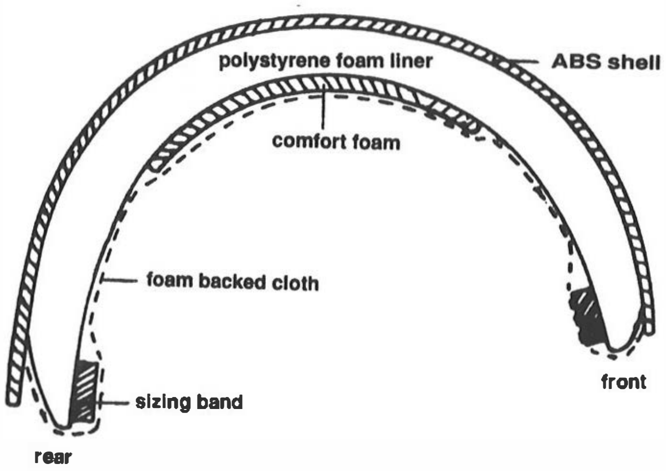

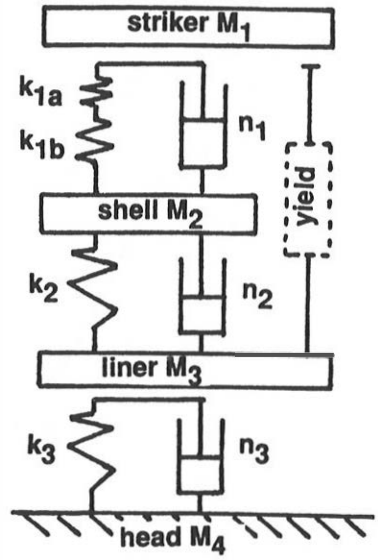

Fig. 5. Thermoplastic motorcycle helmet a) construction b) modelling for an impact.

once a buckling force Fb of the order of 1 kN is exceeded. If a viscous damper n_1 is placed in parallel with this buckling spring, to introduce the viscoelastic nature of the shell, then the dashed curve is predicted for an impact on the shell alone. This response is close to that observed for a hemispherical striker on a shell which had the liner removed locally below the impact point (2). It is difficult to generate data for the local bending of the shell when it impacts a flat surface.

The shock-absorbing liner of the polystyrene foam of density in the range 50 to 90 kg m^{-3} is usually 25 to 35 mm thick. This material has a compressive yield stress in the range 0.5 to 1.2 MNm^{-2} (2), and once the cell walls buckle to allow the compressive deformation they stay permanently buckled. In reality the compressive yield stress increases somewht with increasing strain; fig. 7 shows compressive stress strain curves on foam of density 56 kg m^{-3} for impacts of increasing severity. In the modelling we assume a constant yield stress until a strain of 80%. In a helmet impact we do not have the situation of a rectangular block of foam being compressed between two flat planes. Rather the helmet surface is spherical with radius R, and the impacted surface may also be curved. For an impact with a flat surface the contact area of the liner is 2π Ry where y is the compressive deformation at the initial impact point. Therefore while the liner is being loaded the force F is given by:

$$F = 2\pi RCy$$

where C is the compressive yield stress of the foam. On unloading the crushed foam behaves elastically with a high stiffness. Figure 6b shows the assumed liner compressive response allowing for the increase in contact area with deformation y. Once the deformation approaches the liner thickness and the compressive stran exceeds 80% a sharply rising term $\exp(Ay^2)$ is added to model the bottoming-out. This behaviour is close to that measured experimentally (2).

Finally there is a soft comfort foam inside the helmet that is 3 to 6 mm thick. There is usually also a horizontal sizing band of semi-soft foam, that is of different thicknesses according to the helmet size required. These soft foams have very low stiffnesses k_3, and relatively high damping n_3. When fully compressed they act as rigid solids. Therefore the simulation of their force deflection behaviour (fig. 6c) must also include a sharply rising term $\exp(By^2)$ when the compressive strain exceeds 60%.

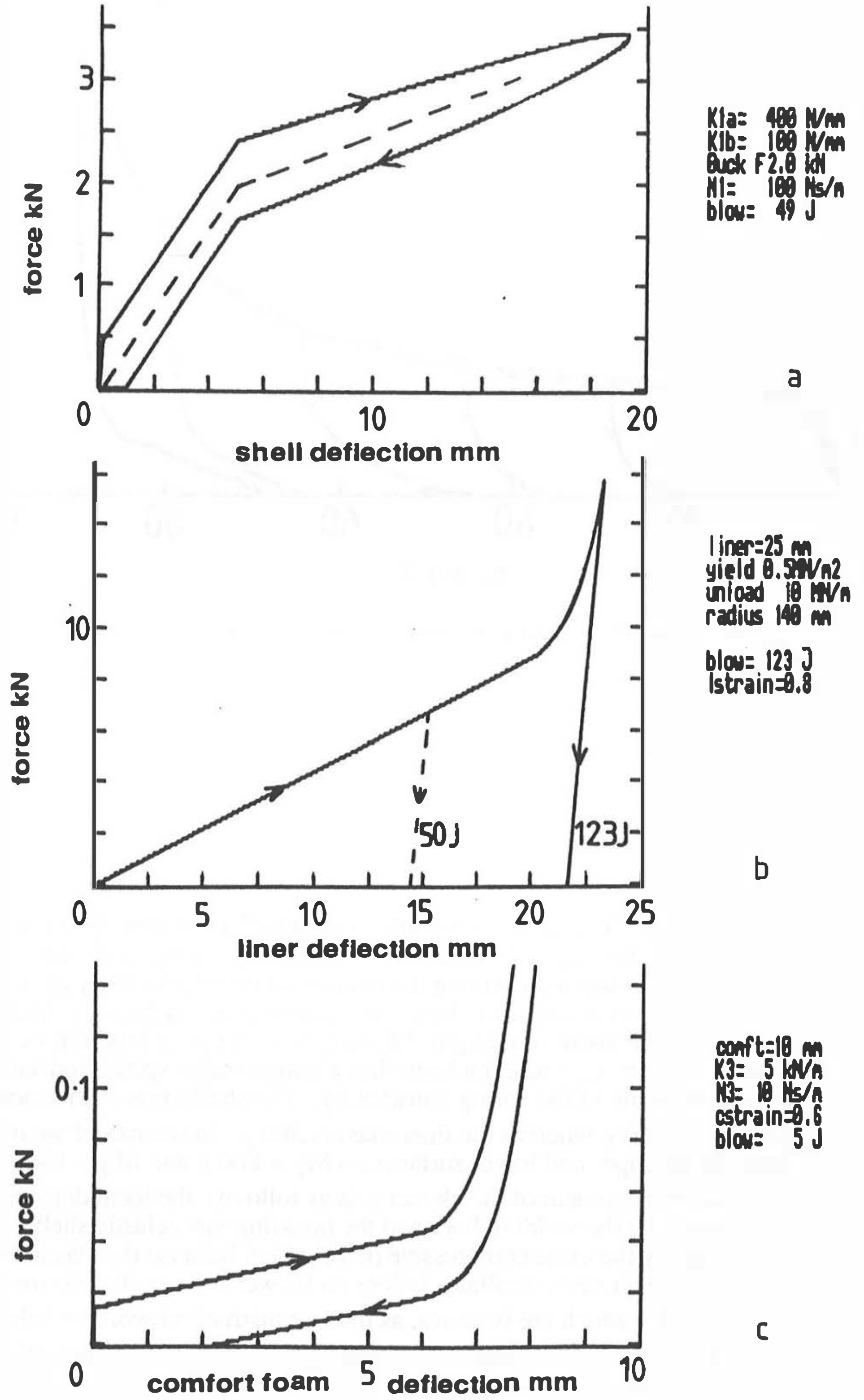

Fig. 6. Modelling the force vs deflection characteristics of the a) shell b) polystyrene foam liner c) comfort foam of a motor cycle helmet.

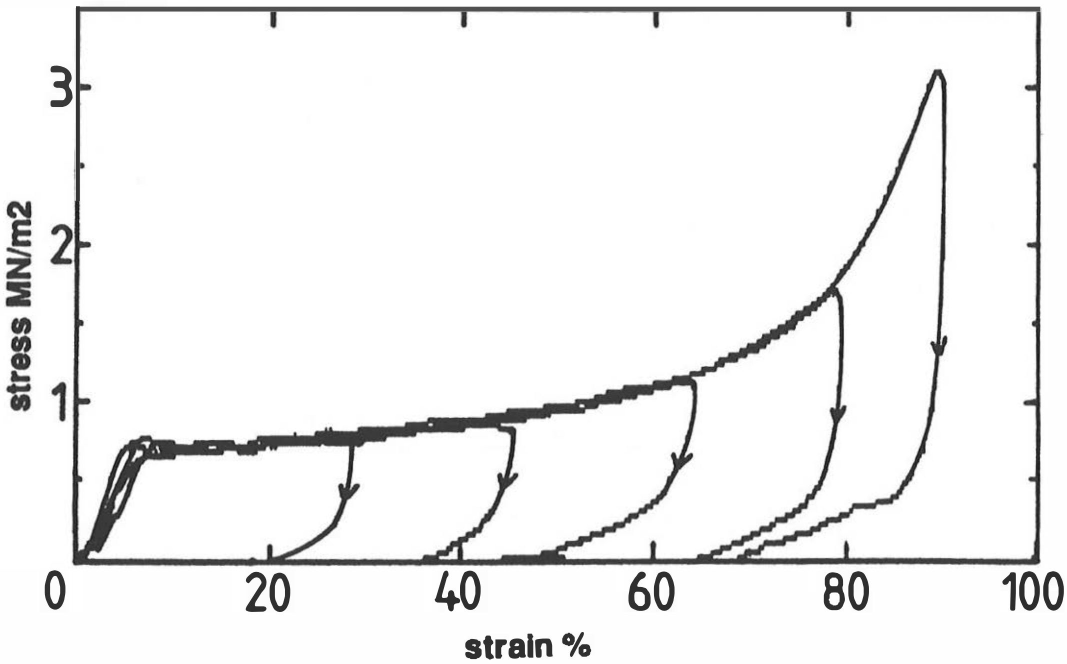

Fig. 7. Set of compressive stress strain curves for polystyrene foam impacted from different heights.

Modelling

Figure 5b shows the model used. The damped non-linear springs for the shell bending, and comfort foam compression have already been described, as has the yielding of the liner. The remaining element is a damped spring representing the uncrushed liner foam away from the impact point. This foam deforms by a combination of shear and compression; its spring constant is estimated as follows: polystyrene foam of 60 kgm^{-3} density has a Youngs modulus of 10 MNm^{-2} (2), a block of 100 mm x 100 mm x 25 mm thickness has a compressive spring constant of 4 MN/m. This is used as an estimate of the spring constant k_2. The shell mass of thermoplastic open face helmets is typically 700 g whereas the liner mass is 200 g. In the model we divide the liner mass equally between its upper and lower surfaces so M_2 = 800 g and M_3 = 100 g. The reason for the series/parallel arrangement of the elements is as follows: the local deformation under the impact point is represented by the yielding liner and the buckling viscoelastic shell in parallel. Both elements experience nearly the same compressive deformation because the elastic liner stiffness k_2 is so large. If the shell mass oscillates it does so between the shell deformation spring k_1 and the elastic liner spring k_2 which are in series, as in the construction workers helmet model. An oscillatory force of 4 kN will only compress the spring k_2 by 1 mm, which is small compared with the shell deformation which can easily be 20 mm. Finally the comfort foam spring k_3 is in series with the other elements as all forces must be transmitted through the comfort foam to the head.

The computation method is the same as that described in section 2. Figure 8a shows the time dependence of both the striker and head forces, for the computer simulation with the following parameters: 122 J impact of 5 kg mass, a shell with $M_2 = 800$ g, $k_{1a} = 400$ kN/m, $k_{1b} = 100$ kN/m, $F_b = 2$ kN, a 25 mm liner of yield stress 0.5 MNm^{-2}, $M_3 = 100$ g, R = 140 mm, $k_2 = 4$ MN/m, $n_2 = 1$ kNs/m, and 5 mm of comfort foam with $k_3 = 5$ kN/m, $n_3 = 10$Ns/m. The predictions include a maximum head force of 14.0 kN, a maximum striker force of 10.4 kN, a maximum liner compression 21.6 mm, and 33 J energy returned to the rebounding striker.

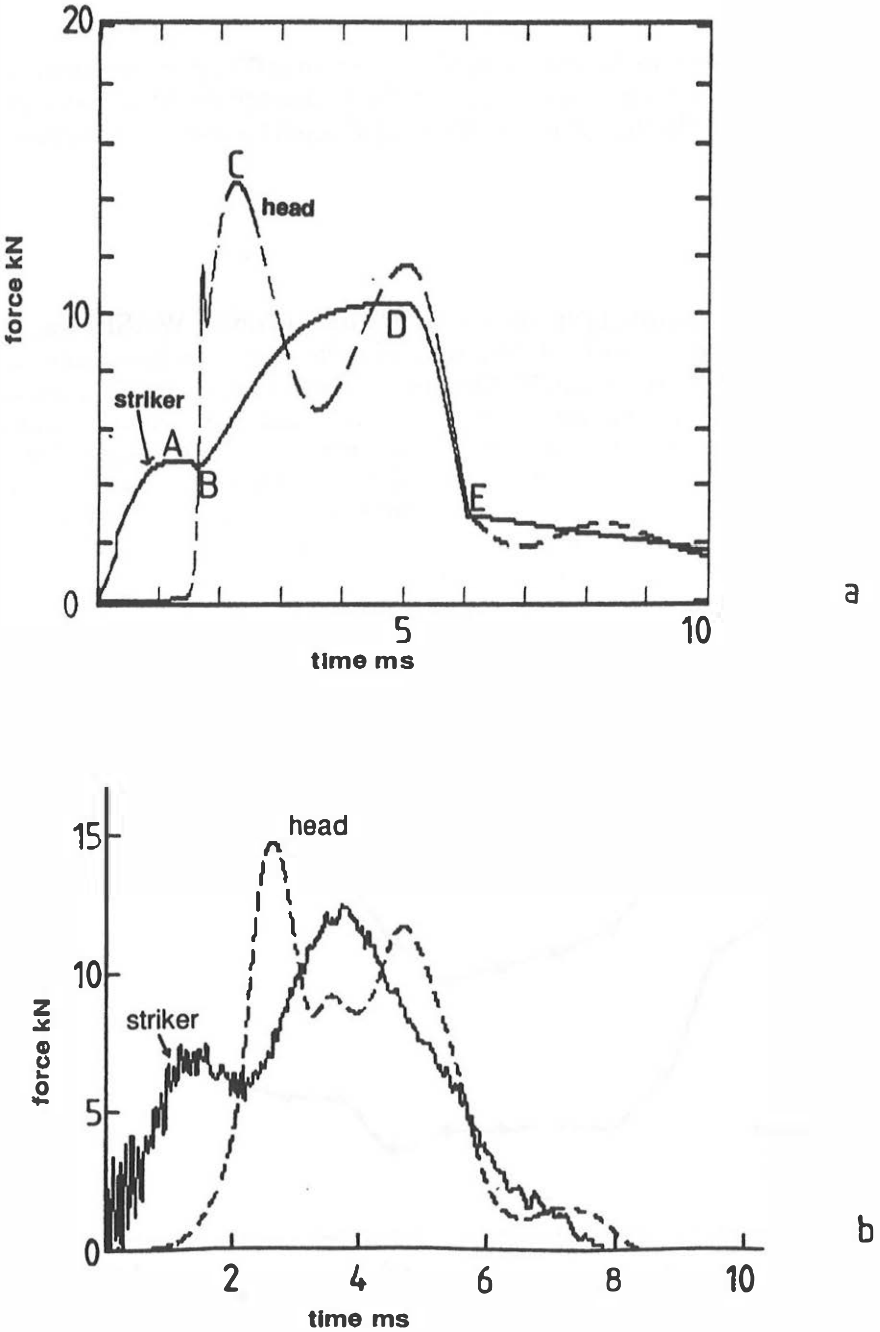

Fig. 8. Striker and head forces vs time for a) computer simulation b) experimental impacts of a flat striker on the top of an open face motorcycle helmet.

Other outputs of the positions versus time allow the interpretation of the force curves. When the striker hits the helmet the force F builds up to a maximum at A as the helmet accelerates. After 1.8 ms at B the 5 mm thick comfort foam is fully compressed and the head force rises rapidly. The shell mass M_2 decelerates to rest after 2.2 ms producing the head force peak C; a large part of this force is transmitted through the elastic part of the liner. The liner then begins to yield under the impact point and after 5.0 ms at D the striker force is a maximum and the liner compression is a maximum of 21.6 mm. The rapid decrease in the forces to E is a result of the elastic unloading of the crushed liner as the striker rebounds upwards, followed by a slower decline in forces as the shell unbuckles.

Experimental data for 122 J falling weight impact on the top of an ABS open face helmet is shown in figure 8b. The fixed headform rested on a load cell so the headforce could be measured (2). There is good agreement between the details of the traces of figures 8a and 8b, apart from the shape of the striker peak D.

High Speed Photography

A second type of open face ABS thermoplastic motorcycle helmet (Toptek WASP) was impacted with a hemispherical striker on the top with 98 J energy. Fig. 9a shows the position of the striker and of the bottom of the shell versus time, and 9b the striker force versus time. The two distinct peaks in the striker force correspond to changes in slope of the striker position versus time. The first peak accelerates the shell towards the headform; subsequent modelling suggest that there was a 10 mm comfort foam plus air gap between the inside of the helmet liner and the headform. The second peak force crushes the liner and buckles the shell inwards. In contrast with the industrial helmets which deformed in overall shape during the impact, the motorcycle helmet only deformed in shape close to the impact site. Thus about 90% of the helmet remains rigid and can be modelled as a concentrated mass, whereas the deformation processes occur in a small region.

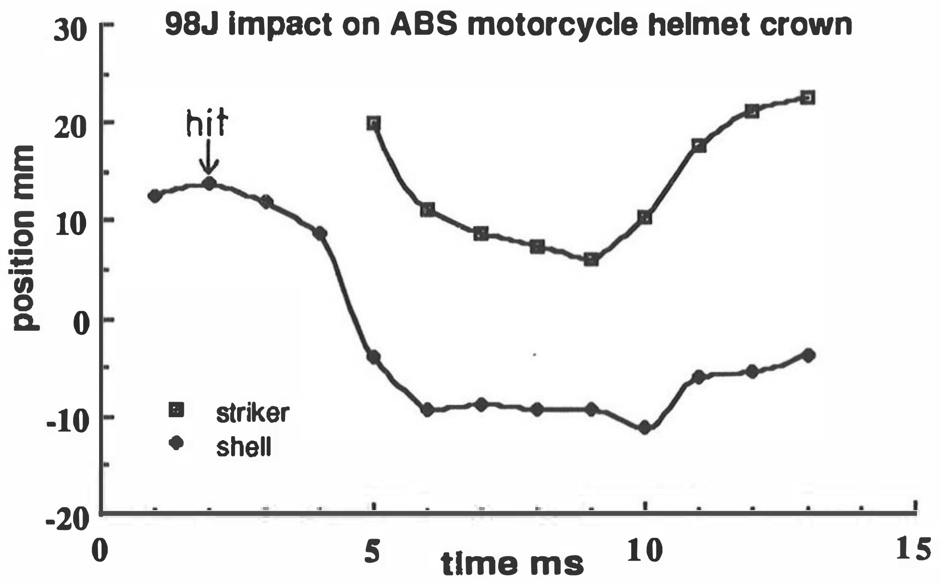

Fig. 9. a) positions of striker and shell from high speed film of 98 J impact of a hemispherical striker on the top of a motorcycle helmet b) striker forces vs time.

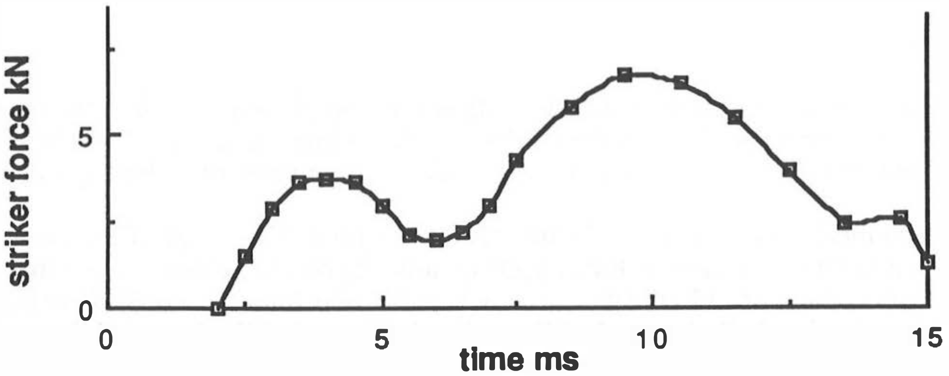

9b

Falling Headform Simulation

Since real motorcycle accidents involve a moving head + helmet, a variant of the model was constructed to consider impacts of a moving 5 kg head with a fixed flat surface. There was relatively little change in the predicted shape of the force time traces compared with fig. 8a. When the impact velocity was varied over the range 1 to 10 m/s the maximum forces on the head and on the flat surface were predicted to vary as in fig. 10. There is a nearly linear increase in the peak forces until a velocity of 8 m/s; at this velocity the liner is crushed by 88% from 25 to 3.0 mm at the maximum deflection. At higher velocities the liner 'bottoms-out' and the forces rise rapidly. It proved difficult to find data to compare with these predictions. Data for impacts of a 5 kg flat striker falling onto a thermoplastic open face helmet on a BS 5361 'swingaway' rig, which the 5 kg headform can move on an arc after impact, gave the relationship

$$F = 1.336\,V - 0.078$$

where F is the peak striker force in kN and V the striker velocity in m/s. For V in the range 4.2 to 9.2 m/s this line fitted the data with a correlation coefficient of 1.00. Compared with impacts of a falling helmetted head onto an infinite mass surface the 'effective impact energy' of the striker in the swingaway test is only 50% of its actual kinetic energy. Consequently the equivalent velocity for the striker is 70.7% of that in fig. 10. When the data is plotted on fig. 10 as peak striker force versus equivalent velocity they confirm the modelling.

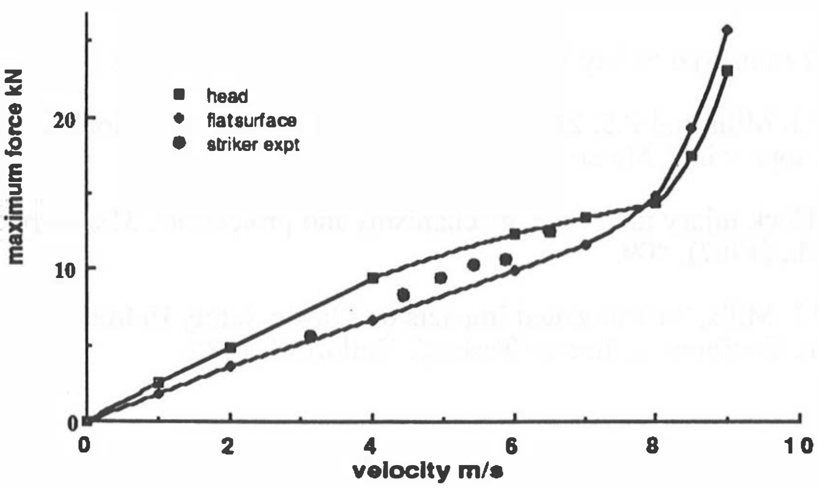

Fig. 10. Predicted peak forces for a 5 kg headform falling onto a flat surface at different velocities. Same helmet parameters as fig. 8, plus experimental striker forces for a thermoplastic helmet tested on a swingaway rig.

4 DISCUSSION

The model for impacts on the top of industrial helmets is very simple but it predicts the main features of experimental impacts. Neither the model, nor the helmet design, is of much use if the impact is to the front or sides of the helmet, as current designs are very much for top impact only.

The one-dimensional model for motorcycle helmets is more complex, but with slight modification it should be able to predict the behaviour for impacts on any site on the helmet. Apart from the masses and dimensions, there are 11 constants to describe the non-linear viscoelastic behaviour of the 4 structural elements: the shell, the crushed liner, the elastic part of the liner and the comfort foam. The significance of several features on impact test traces has been established. In real motorcycle accidents the shell mass oscillations will contribute to the force on the head. The gap between the inside of the liner and the skull may be larger than in these tests because of the presence of the rider's hair, and the force oscillations increase in magnitude with the velocity of impact. Therefore careful design of the softer foams inside helmet may be of major importance in improving helmet performance. It is hoped that the model can be used to optimise the protection afforded by helmets with thermoplastic shells.

ACKNOWLEDGMENT

The research on industrial helmets was funded by the Health and Safety Executive. However the views expressed here are not necessarily those of the Health and Safety Executive.

REFERENCES

1. A. Gilchrist and N.J. Mills, 'Construction site workers helmets', Journal Occupational Accidents, (1987), 8, 199.

2. A. Gale and N.J. Mills, 'Effect of polystyrene foam liner density on motorcycle helmet shock absorption', Plastics & Rubber Proc. & Applic., (1965), 5, 101.

3. H. Kostner and U. Stocker, 'Mathematische Analyse der Stoss absorption im Schutzhelmmaterial', VDI Berichte, (1987), Nr. 657, 211.

4. BS 5240 : 1987 Industrial Safety Helmets. Part 1. British Standards Institution, London.

5. A. Gilchrist, N.J. Mills and P.S. Zhang, 'The effect of contact conditions on impact tests on plastics', to appear in J. Materials Sci.

6. L.M. Patrick, 'Neck injury incidence, mechanisms and protection', 31st Ann. Proc. Amer. Ass. Auto. Med., (1987), 409.

7. A. King and N.J. Mills, 'Instrumented Impacts on Plastic Safety Helmets', Plastics & Rubber Institute Conference, 'Impact Testing', Guildford, 1985.